

**Supporting Information**

**Reduced Polyoxomolybdate Immobilized on Reduced Graphene**

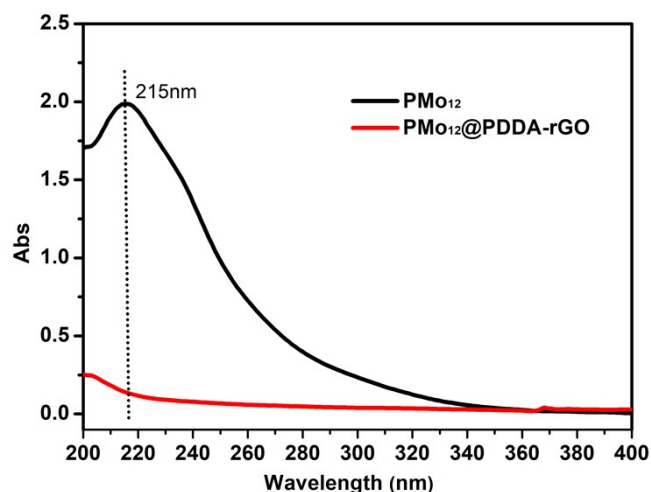
**Oxide for Rapid Catalytic Decontamination of Sulfur Mustard**

**Simulant**

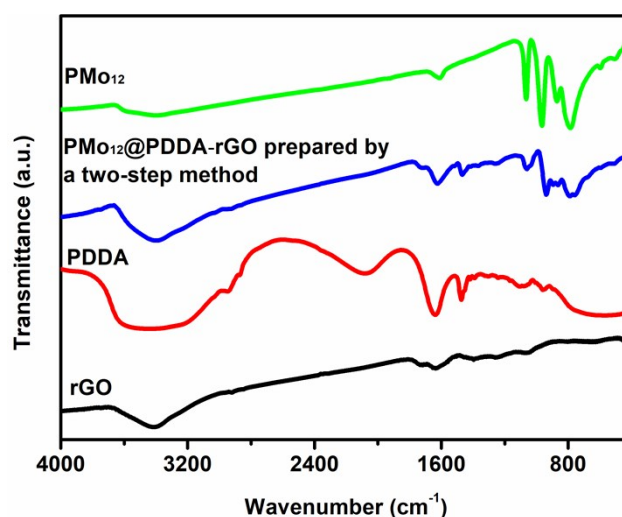
Yanyan Wu<sup>a</sup>, Jing Dong<sup>\*b</sup>, Chengpeng Liu<sup>a</sup>, Xiaoting Jing<sup>a</sup>, Huifang Liu<sup>a</sup>, Yue Guo<sup>a</sup>, Yingnan Chi<sup>\*a</sup>,  
Changwen Hu<sup>a</sup>

<sup>a</sup> *Key Laboratory of Cluster Science Ministry of Education, Beijing Key Laboratory of Photoelectronic/Electrophotonic Conversion Materials, School of Chemistry and Chemical Engineering, Beijing Institute of Technology, Beijing 102488, People's Republic of China.*

<sup>b</sup> *College of Chemistry and Materials Engineering, Beijing Technology and Business University (BTBU), 11 Fucheng Road, Beijing 100048, People's Republic of China.*

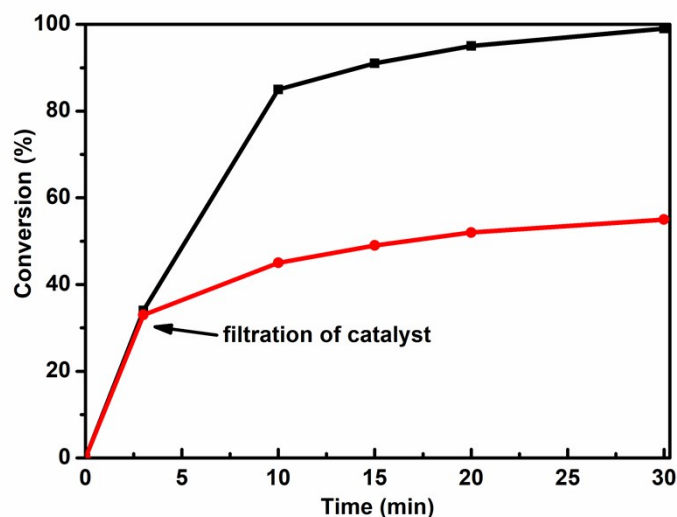


**Figure S1.** Liquid-phase UV-Vis spectrum from leaching test of  $\text{PMo}_{12}@PDDA\text{-rGO}$  immersed in water for 12 h.

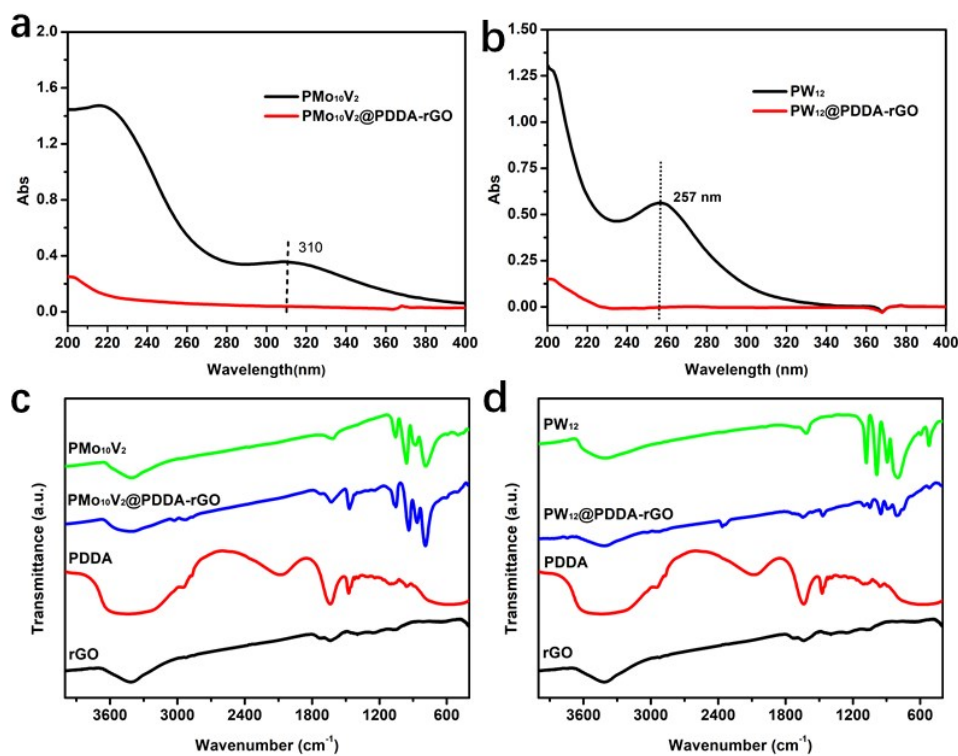


**Figure S2.** FT-IR spectra of  $\text{PMo}_{12}@PDDA\text{-rGO}$  prepared by a two-step method, rGO, PDDA and  $\text{PMo}_{12}$ .

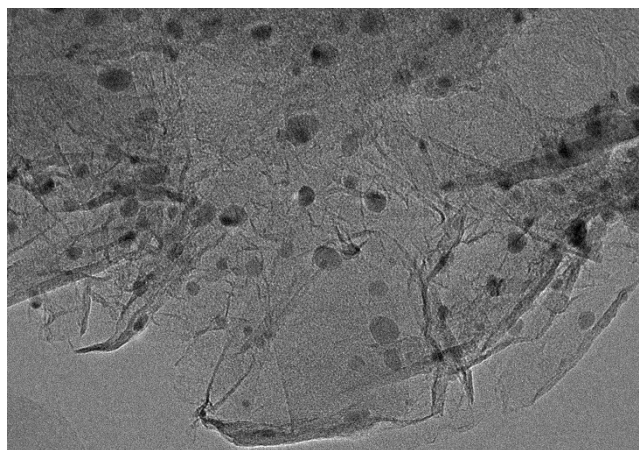
$\text{PMo}_{12}@PDDA\text{-rGO}$  prepared by a two-step method as follows. The mixture of PDDA (0.3 mL) and GO (2 mg/mL, 15 mL) was first treated under hydrothermal conditions (100 °C) for 10 h, and then the resulting PDDA-rGO was dispersed in the aqueous solution of  $\text{PMo}_{12}$  (5 mmol/L, 10 mL). The reaction mixture was stirred for 5 h at room temperature, and the solid product was separated by centrifugation, and washed with deionized water for several times to remove any unloaded  $\text{PMo}_{12}$ . The obtained product was frozen in liquid nitrogen and dried in freeze dryer for two days.



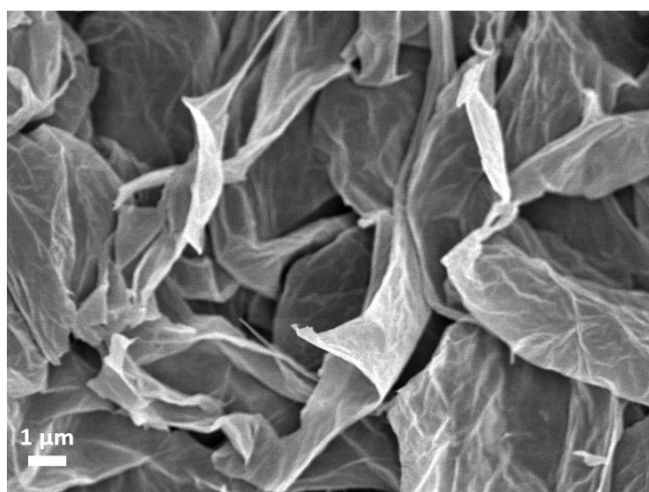
**Figure S3.** Leaching test for CEES degradation using  $\text{PMo}_{12}@PDDA\text{-rGO}$  prepared by a two-step method.



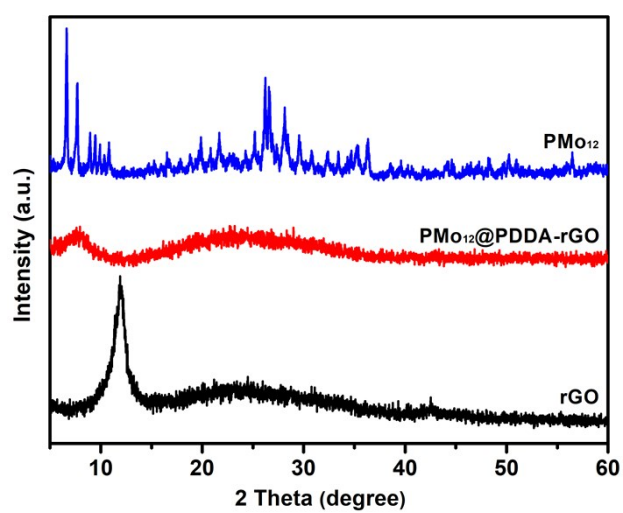
**Figure S4.** Liquid-phase UV-vis spectra from leaching test of (a)  $\text{PMo}_{10}\text{V}_2@PDDA\text{-rGO}$  and (b)  $\text{PW}_{12}@PDDA\text{-rGO}$  immersed in water for 12 h; FT-IR spectra of (c)  $\text{PMo}_{10}\text{V}_2@PDDA\text{-rGO}$  and (d)  $\text{PW}_{12}@PDDA\text{-rGO}$ .



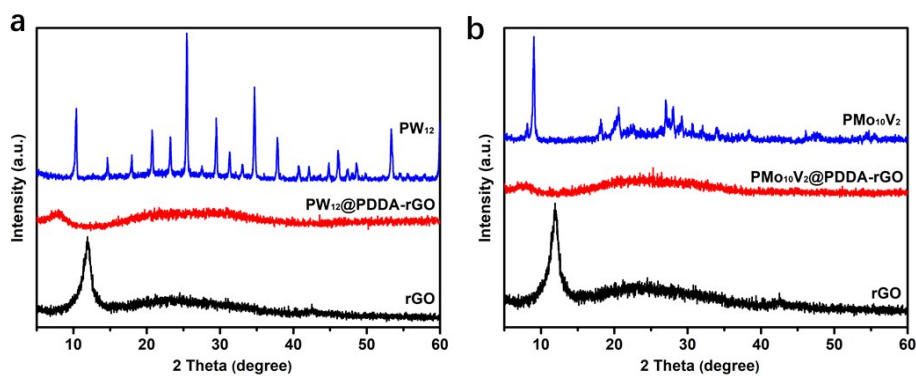
**Figure S5.** TEM image of PMo<sub>12</sub>@PDDA-rGO



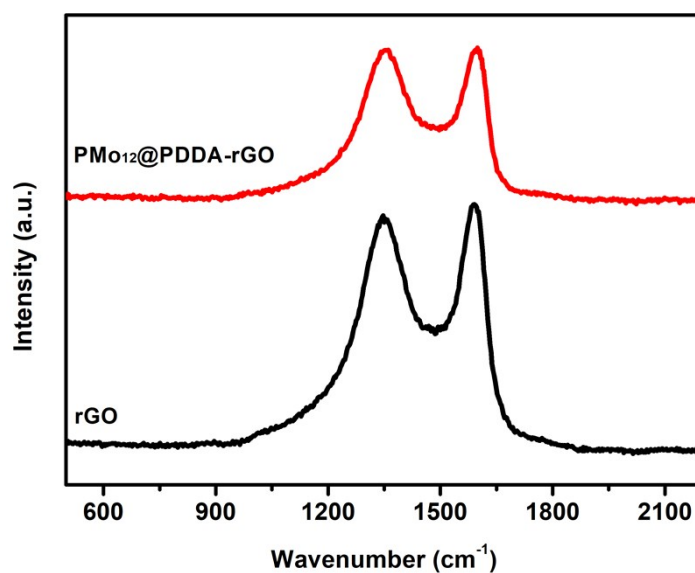
**Figure S6.** SEM image of rGO.



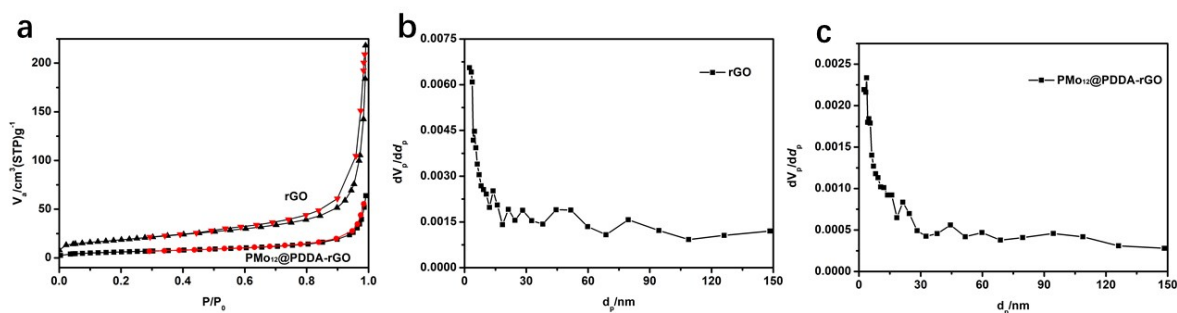
**Figure S7.** PXRD patterns of PMo<sub>12</sub>@PDDA-rGO, PMo<sub>12</sub> and rGO.






**Figure S8.** (a) XRD patterns of  $PW_{12}@PDDA-rGO$ ,  $rGO$  and  $PW_{12}$ ; (b) XRD patterns of  $PMo_{10}V_2@PDDA-rGO$ ,  $rGO$  and  $PMo_{10}V_2$ .



**Figure S9.** Raman spectra of  $PMo_{12}@PDDA-rGO$  and  $rGO$ .



**Figure S10.** (a) The  $N_2$  adsorption-desorption isotherms of  $PMo_{12}@PDDA-rGO$  and  $rGO$ ; Pore size distributions of (b)  $rGO$  and (c)  $PMo_{12}@PDDA-rGO$ .

Sample	Contact angle
PMo <sub>12</sub>	39° 
rGO	70° 
PMo <sub>12</sub> @PDDA-rGO	61° 

**Figure S11.** Contact angle images of PMo<sub>12</sub>@PDDA-rGO, PMo<sub>12</sub> and rGO.

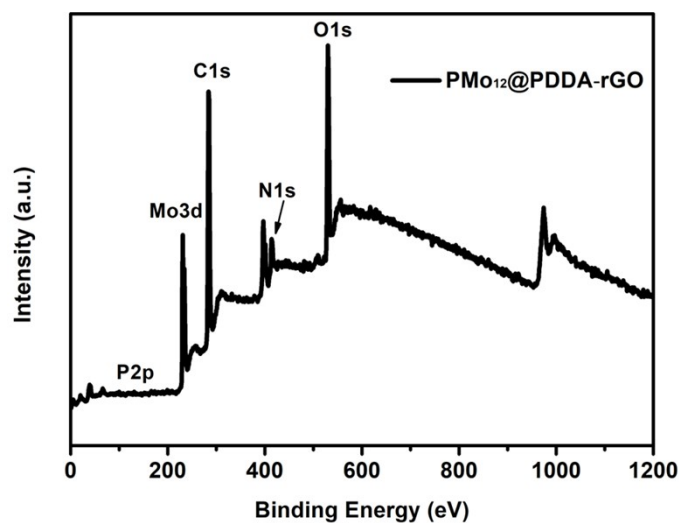


**Figure S12.** XPS survey spectra of PMo<sub>12</sub>@PDDA-rGO.

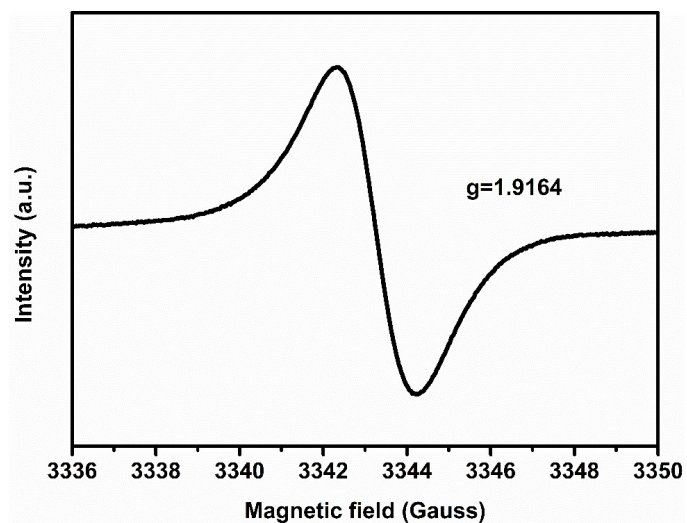


**Figure S13.** EPR spectrum of PMo<sub>12</sub>@PDDA-rGO.

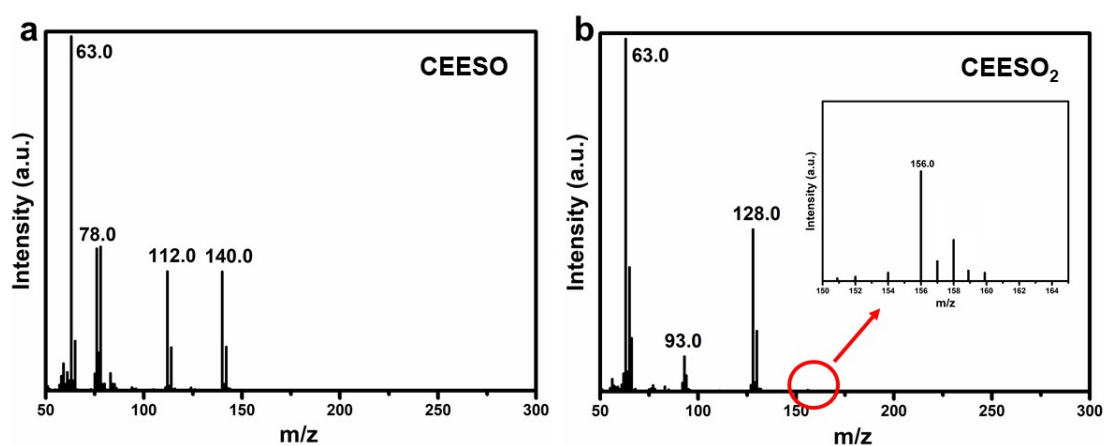


Figure S14. Mass spectrum of (a) CEESO and (b) CEESO<sub>2</sub>.

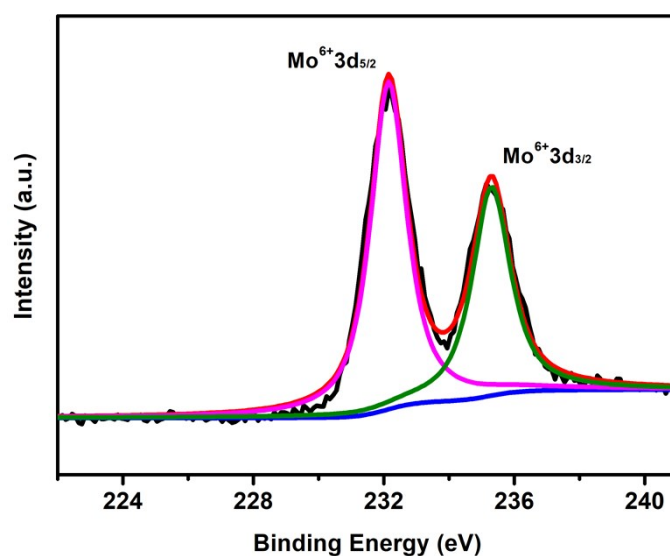


Figure S15. XPS spectra for the Mo3d core level spectrum of PMo<sub>10</sub>V<sub>2</sub>@PDDA-rGO.

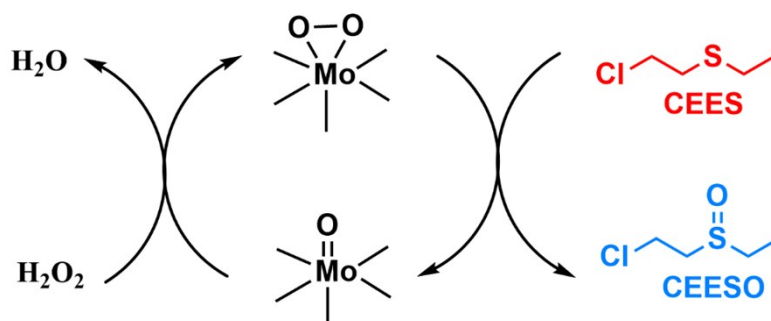


Figure S16. Possible reaction mechanism of CEES decontamination using PMo<sub>12</sub>@PDDA-rGO as catalyst.

**Table S1.** The elemental analysis of PMo<sub>12</sub>@PDDA-rGO.

Sample	Mo(wt%)	P(wt%)	PMo <sub>12</sub> (wt%)
PMo <sub>12</sub> @PDDA-rGO-26%	16.15	0.28	26
PMo <sub>12</sub> @PDDA-rGO-33%	21.10	0.49	33
PMo <sub>12</sub> @PDDA-rGO-45%	28.46	0.82	45
PMo <sub>12</sub> @PDDA-rGO-47%	29.91	0.88	47

**Table S2.** Comparison of the heterogeneous catalysts for the oxidative degradation of sulfur mustard simulant.

Catalyst	Oxidant	Loading (mmol)	TON <sup>[e]</sup>	TOF (min <sup>-1</sup> ) <sup>[f]</sup>	Conv. (%)	Sel. (%) <sup>[a]</sup>	Time (min)	ref.
PMo <sub>12</sub> @PDDA-rGO	3% H <sub>2</sub> O <sub>2</sub>	0.005	49.5	1.7 <sup>[g]</sup>	99	90	30	This work
Mg <sub>3</sub> Al-LDH-Nb <sub>6</sub>	3% H <sub>2</sub> O <sub>2</sub>	0.003	158.3	1.3 <sup>[h]</sup>	95	97	120	1
Zn <sub>2</sub> Cr-LDH-PW <sub>11</sub> Ni	3% H <sub>2</sub> O <sub>2</sub>	0.0015	326.7	1.8 <sup>[i]</sup>	98	94	180	2
Nb <sub>2</sub> O <sub>5</sub>	30% H <sub>2</sub> O <sub>2</sub>	0.075	3.7	0.012 <sup>[j]</sup>	>99	73	300	3
Nb-SAP <sup>[b]</sup>	30% H <sub>2</sub> O <sub>2</sub>	0.0028	95.9	0.2 <sup>[k]</sup>	>98	73	480	4
Fe-DECON1 <sup>[c]</sup>	30% H <sub>2</sub> O <sub>2</sub>	0.043	1.3	0.0009 <sup>[l]</sup>	20	-	1440	5
V-APMS <sup>[d]</sup>	TBHP	0.031	1.3	0.02 <sup>[m]</sup>	97	75.6	60	6
PW <sub>12</sub> @NU-1000	30% H <sub>2</sub> O <sub>2</sub>	0.0017	20.8	10.4 <sup>[n]</sup>	98	57	20	7

[a] The selectivity for CEESO; [b] Nb-SAP: Niobium (V) Saponite Clay; [c] Fe-DECON1: Iron-montmorillonite clays; [d] V-APMS: vanadium-doped acid-prepared mesoporous silica; [e] TON = moles product / moles of total catalytic clusters; [f] TOF = moles product / (moles of total catalytic clusters × amount of time); [g] Time = 90 min; [h] Time = 120 min; [i] Time = 180 min; [j] Time = 300 min; [k] Time = 480 min; [l] Time = 1440 min; [m] Time = 60 min; [n] Time = 2 min.

As shown in Table S2, the TON or TOF of PMo<sub>12</sub>@PDDA-rGO is not better than that of Mg<sub>3</sub>Al-LDH-Nb<sub>6</sub> or Zn<sub>2</sub>Cr-LDH-PW<sub>11</sub>Ni we reported previously. But for the detoxification of chemical warfare agents the decontamination efficiency is a key point to be concern. The decontamination rate of CEES catalyzed by PMo<sub>12</sub>@PDDA-rGO is much better than that by Mg<sub>3</sub>Al-LDH-Nb<sub>6</sub> or Zn<sub>2</sub>Cr-LDH-PW<sub>11</sub>Ni as high POM loading can be achieved with the help of PDDA.

**Table S3.** The oxidative decontamination of CEES catalyzed by PMo<sub>12</sub>@PDDA-rGO



in the presence of radical scavengers.

<b>Radical scavengers</b>	<b>Time (min)</b>	<b>Conv. (%)</b>	<b>Sele. (%)</b>
-	30	98	90
<i>p</i> -benzoquinone ( $\cdot\text{O}_2^-/\cdot\text{O}_2\text{H}$ )	30	97	88
<i>tert</i> -butyl alcohol ( $\cdot\text{OH}$ )	30	98	89
diphenylamine ( $\cdot\text{OH}$ )	30	98	90

Reaction conditions:  $\text{PMo}_{12}\text{@PDDA-rGO}$  (20 mg), CEES (0.25 mmol), 1,3-dichlorobenzene (0.125 mmol), 3 wt% aqueous  $\text{H}_2\text{O}_2$  (internal standard, 0.275 mmol), radical scavengers (0.25 mmol) and acetonitrile (4 mL) at room temperature.

## References

- 1 J. Dong, H. J. Lv, X. R. Sun, Y. Wang, Y. M. Ni, B. Zou, N. Zhang, A. X. Yin, Y. N. Chi and C. W. Hu, *Chem.-Eur. J.*, 2018, **24**, 19208-19215.
- 2 X. R. Sun, J. Dong, Z. Li, H. F. Liu, X. T. Jing, Y. N. Chi and C. W. Hu, *Dalton Trans.*, 2019, **48**, 5285-5291.
- 3 C. Bisio, F. Carniato, C. Palumbo, S. L. Safronyuk, M. F. Starodub, A. M. Katsev, L. Marchese and M. Guidotti, *Catal. Today*, 2016, **277**, 192-199.
- 4 F. Carniato, C. Bisio, R. Psaro, L. Marchese and M. Guidotti, *Angew. Chem. Int. Ed.*, 2014, **53**, 10095-10098.
- 5 F. Carniato, C. Bisio, C. Evangelisti, R. Psaro, V. Dal Santo, D. Costenaro, L. Marchese and M. Guidotti, *Dalton Trans.*, 2018, **47**, 2939-2948.
- 6 C. R. Ringenbach, S. R. Livingston, D. Kumar and C. C. Landry, *Chem. Mater.*, 2005, **17**, 5580-5586.
- 7 C. T. Buru, P. Li, B. L. Mehdi, A. Dohnalkova, A. E. Platero-Prats, N. D. Browning, K. W. Chapman, J. T. Hupp and O. K. Farha, *Chem. Mater.*, 2017, **29**, 5174-5181.